Thin Solid Films 536 (2013) 136–141

Contents lists available at SciVerse ScienceDirect

Thin Solid Films

journal homepage: www.elsevier.com/locate/tsf

Structural anomalies induced by the metal deposition methods in 2D silver nanoparticle arrays prepared by nanosphere lithography

Shengli Huang [a,b,*], Qianqian Yang [a,b], Chunjing Zhang [a], Lingqi Kong [a], Shuping Li [a], Junyong Kang [a]

[a] Fujian Provincial Key Lab of Semiconductors and Applications, Department of Physics, Xiamen University, Xiamen, Fujian 361005, P. R. China
[b] State Key Lab of Silicon Materials, Zhejiang University, Hangzhou 310027, P. R. China

ARTICLE INFO

Article history:
Received 3 July 2012
Received in revised form 2 April 2013
Accepted 3 April 2013
Available online 18 April 2013

Keywords:
Nanosphere lithography
Silver nanoparticle array
Deposition parameter

ABSTRACT

Silver nanoparticle arrays with 2-dimensional hexagonal arrangement were fabricated on the silicon substrates by nanosphere lithography. The silver film was deposited either by thermal evaporation or by magnetron sputtering under different conditions. The nanostructures of the achieved sphere template and the array units were characterized by scanning electron microscopy and atomic force microscopy, and were found to be anomalous under different deposition parameters. Comparative study indicated that the formation of the various 2-dimensional silver nanoparticle array structures was dominated by the thermal energy (temperature), kinetic energy and deposition direction of the deposited metal atoms as well as the size and nanocurvature of the colloidal particles and the metal clusters.

1. Introduction

Metal particles in nanoscale dimension possess many intriguing physical and chemical properties that do not present in their bulk counterpart. The unique properties have received increasing attention in nanotechnology due to their potential application in chemosensors [1], biosensors [2], catalysis [3], photonics [4], data storage [5], etc. Recently, noble metal nanoparticles with 2-dimensional (2D) array structures have been used extensively in biochemical sensors [6–9] for their strong coupling of the electromagnetic wave as characterized by localized surface plasmon resonance (LSPR) among neighbouring particles. The wavelength and intensity of the LSPR spectrum are determined by the shape, size, material, interparticle spacing of the nanoparticles as well as the dielectric constant of the environment. Moreover, the hot spots in the electromagnetic field sensitively rely on the sharp nanoparticle features [10]. Therefore, the ability to produce regular array with designed structures becomes crucial for the LSPR application. A variety of conventional nano-patterning techniques including photolithography [11], electron beam lithography [12], molecular beam epitaxy [13], and nanoimprint lithography [14] have been developed for achieving the 2D nanoparticle arrays. However, these techniques are limited by the drawbacks of slow fabrication speed, low throughput, and high production cost.

As an alternative, nanosphere lithography (NSL) has emerged as a powerful and cost-effective technique that is capable of producing periodic metal particle arrays with controlled shape, size and interparticle spacing [15–18]. It makes use of a template formed by the self-assembly of monodisperse colloidal spheres on flat surface acting as a deposition/etching mask and can be divided into three sequential steps. First, the colloidal spheres self-assemble on a flat surface to form a regular monolayer or multilayer template with a close-packed structure. Next, a thin film with designed metallic type and thickness is deposited onto the sphere mask and the interstices among the spheres. Last, the mask layer is lifted off by etching or dissolution, leaving the metal array units on the substrate. In order to produce regular nanoparticle arrays with designed structures and large enough area, the effect of each preparation parameter on the array structure formation and its mechanism should be clear, and as expected, have drawn much attention in some groups. For example, a huge amount of work has been devoted to the synthesis mechanisms of assembled colloidal spheres [19–21] and organized metallic nanoparticles [22,23]. However, for the thin film deposition in step 2, except the report by M. Ulmeanu et al. [24] that compared the structure differences of the metal arrays using thermal evaporation and magnetron sputtering and concentrated on the deposition direction of the two cases, no papers were found to illuminate the effects of the deposition parameters on the array structure. The variation in the nanoparticle array structure and the mechanism of the array formation as a function of the deposition parameters have yet to be clarified.

With above considerations, in this article, effect of deposition parameters on the silver nanoparticle array structures formation was systematically studied. The silver film was deposited either by thermal evaporation or by magnetron sputtering under different conditions. The nanostructures of the achieved sphere template and the array units were characterized by scanning electron microscopy and atomic force microscopy. With analysis of the relationship between the structural

* Corresponding author at: Fujian Provincial Key Lab of Semiconductors and Applications, Department of Physics, Xiamen University, Xiamen, Fujian 361005, P. R. China. Tel.: +86 592 2186393; fax: +86 592 2189426.
E-mail address: huangsl@xmu.edu.cn (S. Huang).

0040-6090/$ – see front matter © 2013 Elsevier B.V. All rights reserved.
http://dx.doi.org/10.1016/j.tsf.2013.04.006

properties and the deposition parameters, possible mechanisms for the nanostructures formation were revealed.

2. Experimental

The *n*-type silicon wafers with (100) origination and 1–10 Ω cm resistivity were bought from Shanghai Guangwei Electron Material Co., Ltd. The polystyrene (PS) spheres with a mean diameter of 360 nm (coefficient of variation 2.8%) and a concentration of 10 wt% in solution were purchased from Suzhou Nano–Micro Bio-Tech Co. Ltd. For fabricating a large area close-packed nanosphere monolayer as the deposition mask, the silicon wafers were cut into 10 mm × 5 mm pieces as substrates and were thoroughly cleaned in a procedure described elsewhere [25]. The PS solution was diluted to be 3 wt% with deionized water. Subsequently, an 8 μL droplet of the colloidal suspension was deposited onto the silicon substrate with a tilt angle of about 10 degrees off the horizontal to evenly spread the nanospheres solution under the gravity and capillary forces. The specimens were dried in a sealed glass dish overnight.

Silver thin films were deposited in a home-built thermal evaporator and a radio-frequency (RF) magnetron sputter (JS3X-100B, Beijing Chuang Wei Na technology Co., Ltd.). Fig. 1 shows the schematic illustration of the deposition system for the two equipments. For thermal evaporator, the silver granules (99.9%) were placed in a molybdenum disc that faced up directly toward the substrate. The base pressure of the chamber was evacuated to be $P_{TE} = 5.0 \times 10^{-4}$ Pa, and the electric current through the molybdenum disc was increased carefully to be 65 A to achieve a homogeneous deposition rate of $\kappa_{TE} = 2.5$ nm/s when the substrate was seated directly in front of the source material. For RF magnetron sputtering, the thin film was deposited from a silver target (99.99%) in an Ar pressure of 0.76 Pa. The base pressure was reduced to be $P_{MS} = 1.2 \times 10^{-3}$ Pa, and the RF power was set to be 1.5 kW with a frequency of 13.56 MHz to get the deposition rate of $\kappa_{MS} = 0.075$ nm/s. The thickness of the silver films for both the deposition equipments was measured by a surface profiler (Dektak 3 Series) and was controlled to be 100 nm.

To examine the role of deposition parameters on the silver nanoparticle array structure, four different processes were carried out. In Process I and II, the silver films were deposited by thermal evaporation with $\omega_{TE} = 0$ and 16.5 rmp, respectively, and in Process III and IV by magnetron sputtering with $\omega_{MS} = 0$ and 20.0 rmp, respectively. In comparison, for thermal evaporation, the deposited atoms were evaporated directly from the source material to the substrate, which could be regarded as an anisotropic deposition. For RF magnetron sputtering, the deposited atoms were sputtered from the target surface by energetic bombardment of the gas ions (Ar ions in our case). The bombardment might be homogeneous for the target from different directions, thus the sputtering could be considered as an isotropic deposition. In this sense, for Process I, the direction of the evaporating atoms was perpendicular to the PS mask surface, as shown in Fig. 2(a). For Process II, there was a glancing angle between the normal line of the substrate surface and the deposition direction. The glancing angle α might turn from zero to α_M with the frequency of ω_{TE}, as shown in Fig. 2(b) and (c). The α_M value was determined by the distance of S_{TE} and h_{TE} with a relation of $\alpha_M = \arctan\left(\frac{2S_{TE}}{h_{TE}}\right)$, i.e., $0 \le \alpha \le 24.8^0$ for the evaporator. Moreover, the deposition rate was decreased in contrast to the former case as the substrate would move away from the normal line of the molybdenum disc. For Process III and IV, the sputtering atoms were isotropic to the PS mask, as shown in Fig. 2(d). But for Process IV, the rotation of the substrate platform brought a large rate of deposited atoms with bigger glancing angles as the substrates deviated from the target region that had a dense plasma [26].

After the deposition process, the PS spheres were lifted off by sonication in absolute ethanol for 3 minutes. The nanostructures of the PS templates and the silver nanoparticle arrays were characterized by a field-emission scanning electron microscope (SEM, LEO-1530) operated at 20.0 kV and an atomic force microscope (AFM, SPA-400) in a tapping mode.

3. Results

Fig. 3 shows typical SEM images of the PS monolayer template after the silver deposition in the different processes. The colloidal spheres form a hexagonally close-packed monolayer on the substrate in a large scale area (several micrometers in lateral size) for the four specimens. In order to trace the deposition effects on the PS mask, the images of the PS mask boundary in the different processes are only supplied and compared with herein. It can be seen that after the deposition the quasi-triangular spaces among the PS spheres are clearly visible for all of the specimens, which suggests that the gap interspaces

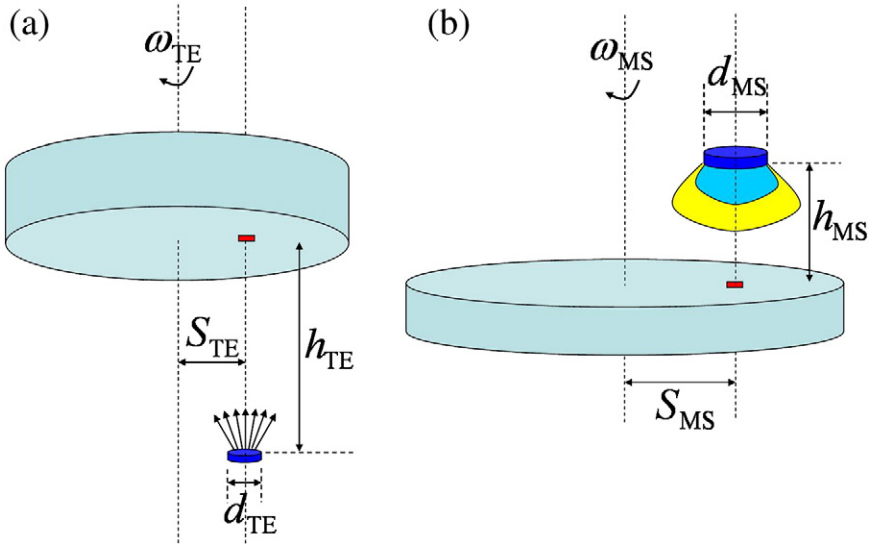

Fig. 1. Schematic illustration of the deposition system for: (a) thermal evaporator and (b) RF magnetron sputter. The values of each parameter are: the diameter of the molybdenum disc diameter $d_{TE} = 10$ mm and of the silver target $d_{MS} = 100$ mm, the distance between the disc (or target) and the substrate platform $h_{TE} = 160$ mm and $h_{MS} = 80$ mm, the distance between the normal line of the disc (or target) and that of the substrate platform $S_{TE} = 37$ mm and $S_{MS} = 160$ mm. The substrate platform can rotate around its normal axis with a modulated frequency ω.